Control Augmented Structural Synthesis with Transient Response Constraints

R. A. Manning* and L. A. Schmit†
University of California, Los Angeles, California

An integrated approach to the optimum design of control augmented structural systems is presented in which structural variables and control variables are changed simultaneously during the design process. Constraints are imposed on peak transient dynamic displacements and accelerations, and control system effort. Side constraints imposed on structural member sizes and control system thresholds and actuator output forces insure the generation of physically meaningful designs. Example problems are presented that illustrate the benefits of simultaneous treatment of both the structural design variables and the control design variables.

Introduction

INTEREST in large flexible space structures has stimulated research efforts aimed at integrating the design of structural and control systems. In many instances, the goal of this integrated design task is to minimize either the total system mass or the control effort expended while satisfying deformation criteria and control system limitations.

In the past, the usual technique for designing these systems has been to fix either the structural or control system design, and redesign the other to improve the fixed system's performance characteristics.[1-3] However, recent investigations[4-6] have shown the synergistic nature of active and passive design techniques. As a result, a number of simultaneous design methods have been suggested in the literature.

These simultaneous structural/control approaches, however, are sequential in nature within an iterative framework. For example, Messac and Turner[7] relate the optimal controls to the structural design variables, and then formulate the design problem in terms of structural variables alone.

A more unified approach to the structural/control design problem has been presented by Junkins et al.[8] and Bodden, Junkins.[9] Their design optimization strategies change both structural (passive) variables and control (active) variables to improve system performance. In Ref. 8, a minimum modification strategy is developed that uses either direct output feedback control or steady-state regulator control in conjunction with two distinct objective functions, namely, eigenvalue placement and minimum control gain Euclidian norm [Eq.(62) of Ref. 8]. In Ref. 9, an eigenspace optimization approach is presented in which structural parameters, sensor/actuator locations, and control feedback gains are included in the set of variables that may be changed during the design process.

A number of authors have recently presented additional integrated structural/control design procedures.[10-12] In all three of these works, the authors address the design problem using linear optimal control laws, with Ref. 12 utilizing (in addition to linear optimal control) a game theory approach to minimize both the weight and the control system energy. Some of the difficulties with linear optimal control are the lack of robustness in system performance due to plant uncertainties and the smearing effect of the performance index to be minimized that could result in larger peak responses.

Previously reported studies, with the exception of Ref. 13, do not include direct consideration of dynamic response constraints and actuator force constraints. The control augmented structural synthesis work reported in Ref. 13 was limited to linear feedback control systems, and it was assumed that the dynamic loading conditions were harmonic, so that steady-state dynamic response was of primary interest. The research results reported here will consider transient dynamic response to arbitrary forcing functions, as well as the use of nonlinear on/off controllers.

In this paper, an integrated approach to control augmented structural synthesis is presented, in which both the structural (passive) variables and the control (active) variables may be changed in order to obtain minimum objective function designs. Constraints on system performance include transient dynamic displacement and/or acceleration constraints, control actuator force upper bounds, control system effort constraints, and a structural mass upper bound. Either structural mass or control effort may be chosen as the objective function to be minimized. The optimum design is found by solving a sequence of explicit NLP problems formed by using a wide range of approximation concepts.

Optimum Design Problem Statement

The design problem posed in the introduction may be stated: Find the vector of design variables $\boldsymbol{d}$, such that some composite objective function, $c_w W + c_e E$, is a minimum and the behavior constraints g_m are satisfied. Mathematically this can be written as: Find the vector $\boldsymbol{d}$ such that

$$\min\ [c_w W(\boldsymbol{d}) + c_e \textstyle\int_0^{t_f} E(\boldsymbol{d},t)\ \mathrm{d}t] \tag{1}$$

subject to

$$g_m(\boldsymbol{d},t) \geq 0 \tag{2}$$

and

$$\boldsymbol{d}^l \leq \boldsymbol{d} \leq \boldsymbol{d}^u \tag{3}$$

where W is the total weight of the structure plus nonstructural masses and E is the control system effort.

The vector of design variables $\boldsymbol{d}$ is made up of beam design element section properties, nonstructural mass design element radii, control actuator thresholds, and output forces. The

Presented as Paper 87-0749 at the AIAA/ASME/AHS/ASEE 28th Structures, Structural Dynamics and Materials Conference, Monterey, CA, April 6-8, 1987; received May 19, 1988; revision received June 5, 1989.

*Graduate Research Assistant; currently Staff Engineer, TRW Space and Technology Group.

†Professor of Engineering and Applied Science. Fellow AIAA.

structure is assumed to have fixed configuration, topology, and material.

The 12-degree-of-freedom box-beam finite elements shown in Fig. 1 are used to model the structures. A number of analysis elements may be linked to a single design element and, additionally, linking of CSDs within the cross section of the design element is allowed. Direct section properties are used as the structural variables in the optimization and CSDs are recovered subsequently.

Nonstructural masses can either be fixed for model definition or be used as independent design elements during the optimum design process. The nonstructural masses (see Fig. 3) consist of spherical elements of specified material and either fixed radii or variable radii (depending on whether the nonstructural masses are used as design elements).

The control system consists of a given number of sensors at specified degrees of freedom and a fixed number of control actuators (thrusters) at specified degrees of freedom. The characteristics of the sensors are invariant during the design process and allow a set of output measurements, Y_n and $\dot{Y}_n$, to be obtained. Based on these output measurements, the actuators produce control forces aimed at reducing dynamic response.

Two different control laws have been used. The first (referred to as type I) uses both displacement and velocity measurements to produce output control forces according to the relation

$$u_n = \begin{cases} 0 \text{ if } |Y_n| \le \delta_n \\ -\bar{u}_n \text{ if } |Y_n| \ge \delta_n \text{ and } Y_n \ge 0 \text{ and } \dot{Y}_n \ge 0 \\ -\bar{u}_n \text{ if } |Y_n| \ge \delta_n \text{ and } Y_n \ge 0 \ge \dot{Y}_n \text{ and } |\dot{Y}_n| \le \epsilon_n \\ +\bar{u}_n \text{ if } |Y_n| \ge \delta_n \text{ and } Y_n \le 0 \text{ and } \dot{Y}_n \le 0 \\ +\bar{u}_n \text{ if } |Y_n| \ge \delta_n \text{ and } Y_n \le 0 \le \dot{Y}_n \text{ and } |\dot{Y}_n| \le \epsilon_n \\ 0 \text{ otherwise} \end{cases} \quad (4)$$

where ϵ_n is the velocity threshold, δ_n the magnitude of the deadband region, and $\bar{u}_n$ the magnitude of the output force. In this instance, the deadband region size δ_n and the output force $\bar{u}_n$ are used as the design variables. Figure 2 graphically shows the actuator forces produced for a typical set of sensor measurements for the type I control law. The second (referred to as type II) uses velocity measurements to produce output forces according to the relation

$$u_n = \begin{cases} 0 \text{ if } |\dot{Y}_n| \le \epsilon_n \\ -\bar{u}_n \text{ if } |\dot{Y}_n| \ge \epsilon_n \text{ and } \dot{Y}_n \ge 0 \\ +\bar{u}_n \text{ if } |\dot{Y}_n| \ge \epsilon_n \text{ and } \dot{Y}_n \le 0 \\ 0 \text{ otherwise} \end{cases} \quad (5)$$

where the velocity threshold ϵ_n and the magnitude of the output force $\bar{u}_n$ are used as the design variables. Figure 3 graphically shows the type II actuator forces produced for the same typical sensor measurements as were used for the type I control law. In either case, a small amount of vibration is tolerable, as indicated by the presence of the deadband region and velocity threshold parameters, but any vibration past this level activates the control system.

The set of constraints g_m contains dynamic displacement and/or rotation constraints and dynamic translational and/or rotational acceleration constraints. It should be noted that all of the behavior constraints represented by g_m are time parametric in nature.

The side constraints in Eq. (3) represent upper and lower bounds on the beam element cross-sectional dimensions that have been transformed to section property side constraints, as well as upper and lower bounds on the nonstructural mass and control system design variables. The side constraints are necessary to satisfy analysis validity limitations in addition to other designer-specified guidelines.

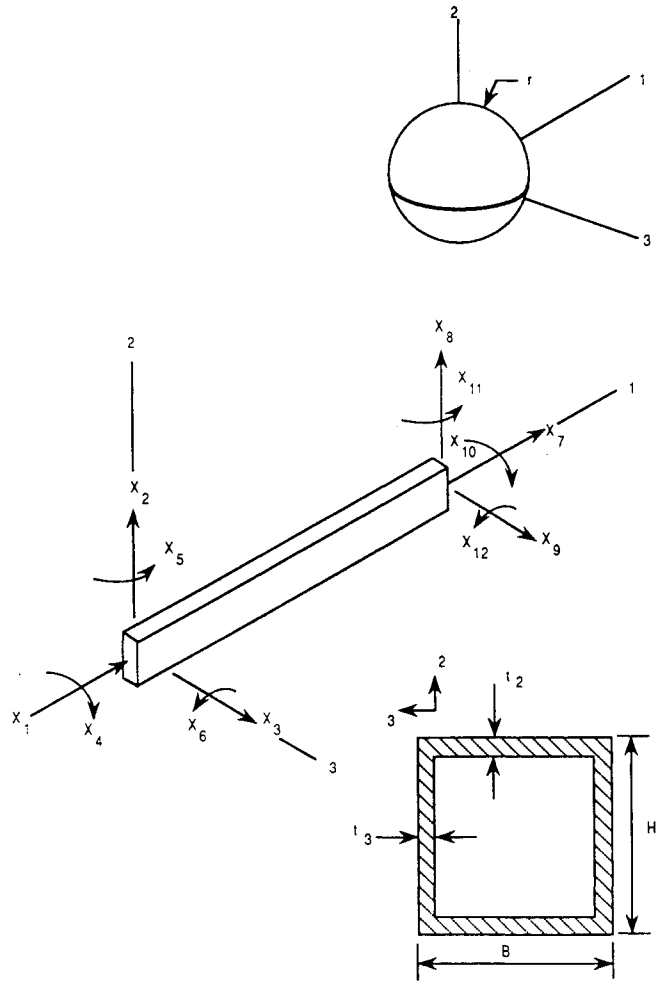

Fig. 1 Structural design elements

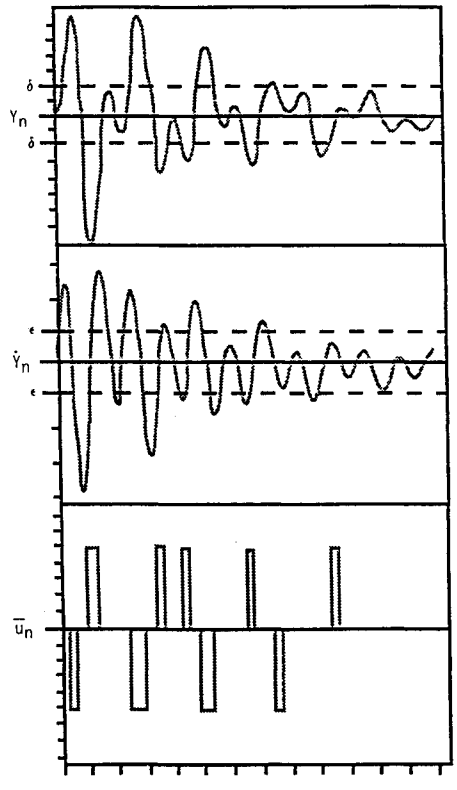

Fig. 2 Type I actuator outputs for typical sensor measurements.

In general, the optimum design problem represented by Eqs. (1-3) is a complex nonlinear mathematical programming problem that precludes direct solution attempts even in the absence of time parametric constraints.[14]

The composite objective function design problem contained in Eqs. (1-3) can be specialized to a weight minimization problem by deleting $E(d,t)$ from Eq. (1) and adding a control effort constraint

$$E^u \geq \int_0^{t_f} E(d,t)\, dt = E(d) \tag{6}$$

or, alternatively, the basic problem statement can be specialized to a minimum control effort problem by deleting $W(d)$ from Eq. (1) and adding a weight constraint

$$W^u \geq W(d) \tag{7}$$

In this paper the approximation concepts approach (e. g., see Refs. 13 and 14) is extended to control augmented structural synthesis problems with time parmetric constraints and nonlinear on/off controllers. This is accomplished by replacing the time parametric constraints with a finite number of regular constraints corresponding to response peaks and then using hybrid approximations (see Ref. 15) to replace these implicit constraint functions with explicit approximations in terms of the design variables. Move limits are used on the design variables to protect the quality of each approximate problem. The approximate form of the weight minimization problem becomes

$$\min\ W(d) \tag{8}$$

subject to

$$\tilde{g}_m(d) \geq 0 \tag{9}$$

$$E^u \geq \tilde{E}(d) \tag{10}$$

and

$$d^l \leq d \leq d^u \tag{11}$$

and the approximate form of the control effort minimization problem becomes

$$\min\ \tilde{E}(d) \tag{12}$$

subject to

$$\tilde{g}_m(d) \geq 0 \tag{13}$$

$$W^u \geq W(d) \tag{14}$$

and

$$d^l \leq d \leq d^u \tag{15}$$

where $\tilde{g}_m(d)$ and $\tilde{E}(d)$ denote explicit hybrid approximations.

Solution of either the weight minimization problem specified in Eqs. (1-3) and (6) or the control effort minimization specified in Eqs. (1-3) and (7) proceeds as a sequence of solutions to approximate problems given by either Eqs. (8-11) or Eqs. (12-15). The steps necessary for the solution of the approximate problem are 1) analysis of the control augmented structure at the current design; 2) evaluation of the behavior constraints; 3) deletion of the non-critical constraints; 4) computation of sensitivities of the retained constraints with respect to all design variables; 5) formation of the explicit hybrid approximations for the current stage; 6) solution of the approximate problem using a nonlinear mathematical programming algorithm, such as the method of feasible directions implemented in CONMIN[16]; and 7) recovery of element physical dimensions from the optimization variables to yield a new current design.

There are a number of advantages to using this type of solution method. First, the method replaces an implicit problem with a sequence of explicit problems. Second, the size of each approximate optimization problem is relatively small due to the use of design element linking and temporary constraint deletion. Third, convergence of the method is rapid, provided a thoughtful choice of intermediate design variables is made so that the approximations are of high quality.

Analysis Methodology

Using a finite-element representation of a control-augmented structure, the system equations of motion can be written as

$$M_{ji}\ddot{X}_i + K_{ji}X_i = P_j + B_{jn}u_n \tag{16}$$

where M_{ji} is the system mass matrix, K_{ji} the system stiffness matrix, P_j the vector of nodal external excitation forces, B_{jn} a matrix of zeroes and ones placing the control actuators at certain preselected nodal degrees of freedom, u_n the vector of actuator force outputs, and X_i the vector of nodal displacements and rotations. In the transient dynamic case, the external forces, the actuator force outputs, and the nodal displacements and rotations are all time dependent.

Vectors of observed displacements and velocities, Y_n and $\dot{Y}_n$, respectively, are available from the control system sensors, and are given by

$$Y_n = C_{ni}X_i \tag{17}$$

and

$$\dot{Y}_n = C_{ni}\dot{X}_i \tag{18}$$

where C_{ni} is a matrix of zeroes and ones locating the control sensors at nodal degrees of freedom.

The normal mode method of analysis[17] is used to obtain the time dependent displacements, velocities, and accelerations that ate solutions to Eq. (16). The normal mode method

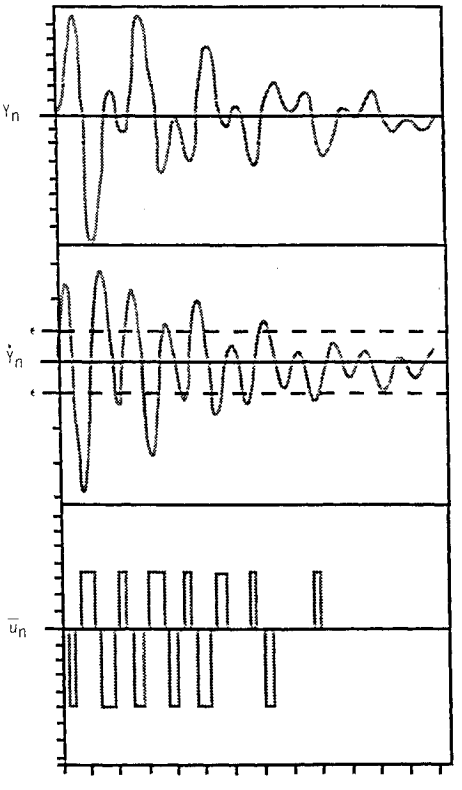

Fig. 3 Type II actuator outputs for typical sensor measurements.

consists of two basic steps: 1) uncoupling of the equations ofmotion by using the system eigenvalues and eigenvectors and 2) time stepping for the dynamic modal response followed by transformation back to the physical degrees of freedom.

The normal mode method of analysis is based on the use of a modal transformation

$$X_i = \phi_{ik} q_k \tag{19}$$

where the modal matrix ϕ_{ik} is a matrix of spatial patterns and the modal response q_k is a vector of time dependent normal coordinates.

Introduction of the modal transformation given by Eq. (19) into Eq. (16), and premultiplication by the transpose of the modal matrix yields

$$\ddot{q}_k + 2\zeta_k \omega_k \dot{q}_k + \omega_k^2 q_k = Q_k + Z_k \tag{20}$$

where the vector of modal excitation forces Q_k is given by

$$Q_k = \phi_{jk} P_j \tag{21}$$

and the vector of modal control forces Z_k is given by

$$Z_k = \phi_{jk} B_{js} u_s \tag{22}$$

and ζ_k and ω_k are the kth modal damping ratio and kth natural frequency, respectively.

Solution for the modal response from Eq. (20) proceeds very rapidly with the use of the Wilson-θ time stepping method.[18] The Wilson-θ method is an explicit time integration method that is unconditionally stable for any time step size, provided that the θ parameter is greater than 1.37. Physical degree-of-freedom responses can be obtained at each time step using the modal transformation in Eq. (19).

Behavior constraints are readily evaluated from the peak physical degree-of-freedom responses, and noncritical constraints can now be deleted from further consideration during the current approximate problem solution.

Calculation of Sensitivities

Time parametric peak transient displacement and acceleration sensitivities can be obtained by differentiating the modal transformation in Eq. (19) to give

$$\frac{\partial X_i}{\partial d_r} = \frac{\partial \phi_{ik}}{\partial d_r} q_k + \phi_{ik} \frac{\partial q_k}{\partial d_r} \tag{23}$$

and

$$\frac{\partial \ddot{X}_i}{\partial d_r} = \frac{\partial \phi_{ik}}{\partial d_r} \ddot{q}_k + \phi_{ik} \frac{\partial \ddot{q}_k}{\partial d_r} \tag{24}$$

The difficult terms to obtain, $\partial q_k/\partial d_r$ and $\partial \ddot{q}_k/\partial d_r$, can be computed in an efficient manner by writing the modal equations of motion in first-order form as

$$\begin{bmatrix} \dot{\eta}_1 \\ \dot{\eta}_2 \end{bmatrix} = \begin{bmatrix} 0 & 1 \\ -\alpha_1 & -\alpha_2 \end{bmatrix} \begin{bmatrix} \eta_1 \\ \eta_2 \end{bmatrix} + \begin{bmatrix} 0 \\ 1 \end{bmatrix} Q + \begin{bmatrix} 0 \\ 1 \end{bmatrix} Z \tag{25}$$

where it is understood that $\eta_1 = q$, $\eta_2 = \dot{q}$, and the essential parameters are defined as $\alpha_1 = \omega^2$ and $\alpha_2 = 2\zeta\omega$. Now rewrite Eq. (25) in compact form

$$\dot{\eta} = \bar{A}\eta + bQ + bZ \tag{26}$$

and apply the Wilkie-Perkins[19] essential parameter method. The Wilkie-Perkins essential parameter method takes advantage of the special form of the $\bar{A}$ matrix to reduce the amount of time stepping needed in calculating the time parametric transient response sensitivities.[20] In this manner, the sensitivities are obtained by 1) time stepping K sets of Eq. (27)

$$\frac{\partial \dot{\eta}}{\partial \alpha_1}\Big|_{t+\Delta t} = [\bar{A}] \frac{\partial \eta}{\partial \alpha_1}\Big|_t + \left[\frac{\partial \bar{A}}{\partial \alpha_1}\right] \eta|_t \tag{27}$$

2) utilizing the relations

$$\frac{\partial \eta_1}{\partial \alpha_2} = \frac{\partial \eta_2}{\partial \alpha_1} \tag{28}$$

and

$$\frac{\partial \eta_2}{\partial \alpha_2} = -\eta_1 - \alpha_1 \frac{\partial \eta_1}{\partial \alpha_1} - \alpha_2 \frac{\partial \eta_2}{\partial \alpha_1} \tag{29}$$

and 3) transforming essential parameter sensitivities to design variable sensitivites by

$$\frac{\partial}{\partial d_r} = \frac{\partial \alpha_1}{\partial d_r} \frac{\partial}{\partial \alpha_1} + \frac{\partial \alpha_2}{\partial d_r} \frac{\partial}{\partial \alpha_2} \tag{30}$$

The computational effort required will now be that needed for time stepping solutions of K sets of Eq. (25) for the system response and K sets of Eq. (27) for the modal response sensitivities, where K is the number of retained modes.

It should be noted that this method of obtaining sensitivities can only be used for the passive structural design variables because the essential parameters, α_1 and α_2, are independent of the active control design variables. For the active control variables, the sensitivity equations are obtained by differentiating Eq. (26) with respect to the control design variables to yield

$$\frac{\partial \dot{\eta}}{\partial d_r}\Big|_{t+\Delta t} = [\bar{A}] \frac{\partial \eta}{\partial d_r}\Big|_t + b \frac{\partial Z}{\partial d_r}\Big|_t \tag{31}$$

Active control sensitivities are obtained using the finite difference method on Eq. (31) because of the complex form of the control laws.

The Wilkie-Perkins essential parameter method is well suited for further efficiency improvements if parallel processing facilities are available, since the sensitivity of each mode is calculated independently of all other modes.

Once the sensitivities have been obtained, peak response constraints are approximated using the results of the time parametric sensitivity analysis. Each approximate problem is solved using CONMIN,[16] and then the cross-sectional dimensions corresponding to the final values of the direct section properties are obtained using a linearized recovery scheme.[14]

Numerical Examples

In this section, numerical results for some example problems are presented. The problems were solved using a research-level computer code originally written on an IBM AT personal computer and modified to run on an FPS-164 computer.

Planar Grillage Structure—Case 1

The 21-degree-of-freedom planar grillage structure shown in Fig. 4 will be used here for examples where weight minimization is selected as the design objective. The structural material is taken to be aluminum (see Table 1 for material properties), and the grillage is subjected to the transient force-time history shown in Fig. 4. The load is applied at node 8, slightly off the centerline of the structure, so that both symmetric and nonsymmetric modes are excited. Behavior constraints are placed on the vertical dynamic displacement at nodes 2, 4, 5, 6, and 7 (see Table 1 for specific limiting values). The dynamic analyses for all planar grillage examples (cases 1–4) were carried out using 10 retained modes (frequency content up to 100 Hz), a final integration time of 1.0 s, a time

Table 1 Planar grillage example input data

Material properties:	$E = 7.3 \times 10^{10}$ N/m^2 $\rho = 2770$ kg/m^3 $\nu = 0.325$
Loading:	(See Fig. 4)
Dynamic constraints:	$\lvert X_{y2}, X_{y4}\rvert < 7.5 \times 10^{-4}$ m $\lvert X_{y5}, X_{y6}\rvert < 9.0 \times 10^{-4}$ m $\lvert X_{y7}\rvert < 9.0 \times 10^{-4}$ m $\lvert \ddot{X}_{y2}, \ddot{X}_{y4}\rvert < 7.5$ m/s^2 $\lvert \ddot{X}_{y5}, \ddot{X}_{y6}\rvert < 9.0$ m/s^2 $\lvert \ddot{X}_{y7}\rvert < 9.0$ m/s^2
Control constraints:	$E < 55.0\ N^2 - s$
CSD variable linking:	$B,H = 0.5$ m fixed, $t_2 = t_3$ $\epsilon = 0.01$ m/s fixed (Type I only)

Side constraints

Variable	Units	Lower bound	Initial design	Upper bound
B	m	0.10	0.50	2.00
H	m	0.10	0.50	2.00
t_2	m	0.001	0.005	0.02
t_3	m	0.001	0.005	0.02
r	m	0.1	0.1	2.0
δ	m	0.0001	0.0002	0.0008
ϵ	m/s	0.001	0.005	1.00
$\bar{u}$	N	0.1	5.0	10.0

step size of 0.0005 s, and 2% modal damping (i.e., $\zeta = 0.02$). All relevant input information is shown in Table 1.

The minimum weight design of this structure is sought for the uncontrolled case, for the controlled case using one collocated sensor/actuator at node 6, and for the controlled case using two collocated sensor/actuators located at nodes 5 and 7. All controlled cases were run using both the type I actuators and the type II actuators. However, superior performance was achieved in all cases using the type II actuators, hence type I actuator results will not be reported here for the planar grillage (see Ref. 21 for type I results).

Table 2 contains the optimum design and the critical constraints for all of these subcases. A minimum mass of 538 kg was obtained for the optimum design of the uncontrolled structure. Because the structure acts primarily like a cantilever, design elements 3, 4, and 5 reach their minimum gage thicknesses at the optimum design and the dynamic displacements at nodes 6 and 7 reach their upper limit. The optimum design tapers down from root to tip, as expected.

Table 2 contains the optimum design and the critical constraints for the uncontrolled design, single type II actuator controlled design, and two type II actuator controlled designs. At the optimum design for each design problem, an analysis convergence check was done to insure that the number of modes retained and time step size were adequate to accurately capture the dynamic response.

The optimum design for the single type II actuator controlled design is 346 kg, 30.2% lighter than the uncontrolled optimum design. The critical constraints, namely the dynamic displacement at node 7, the actuator force upper bound, and the lower bound beam thickness dimensions for design elements 3, 4, and 5, suggest that bending effects are being controlled. However, torsional effects cannot be controlled, due to the location of the actuator on the center line of the structure.

Simultaneous bending-torsion control was attempted using two type II actuators, one at node 5 and one at 7. The two type II actuator subcases yield a minimum mass of 259 kg, 51.9% lighter than the uncontrolled minimum mass design. The critical constraints are the dynamic displacement at node 6, the actuator force upper bound for the actuator at node 7, and the beam thickness lower bounds for design elements 2, 3, 4, and 5. This critical constraint combination implies that control of the torsional effects can be achieved in conjunction with control of the bending effects by using two type II actuators. It is observed that the actuator force at node 7 reaches its upper bound, thereby reducing the torsional effects of the excitation, and letting both actuators combine to reduce the bending effects.

Table 2 Planar grillage optimal designs—case 1 (Type II actuators)

Design variables	Units	Uncontrolled (1A)	1 Type II actuator (1D)	2 Type II actuators (1E)
Beam 1 t	m	0.0060	0.0025	0.0012
Beam 2 t	m	0.0015	0.0014	0.0010
Beam 3 t	m	0.0010	0.0010	0.0010
Beam 4 t	m	0.0010	0.0011	0.0010
Beam 5 t	m	0.0010	0.0010	0.0010
Node 5 ϵ	m/s	—	—	0.0016
Node 5 $\bar{u}$	N	—	—	7.79
Node 6 ϵ	m/s	—	0.0024	—
Node 6 $\bar{u}$	N	—	10.00	—
Node 7 ϵ	m/s	—	—	0.0024
Node 7 $\bar{u}$	N	—	—	10.00
Total mass	kg	538	346	259
Iterations		15	14	13
Critical constraints		t_3^-,[a] t_4^-, t_5^- X_{y6},[c] X_{y7}[c]	t_3^-, t_5^-, u_6^+[b] X_{y7}[c]	t_2^-, t_3^-, t_4^- t_5^-, u_7^+, X_{y6}[c]

[a]:Design variable at lower bound. [b]:Design variable at upper bound. [c]Subscripts on u indicate nodal locations.

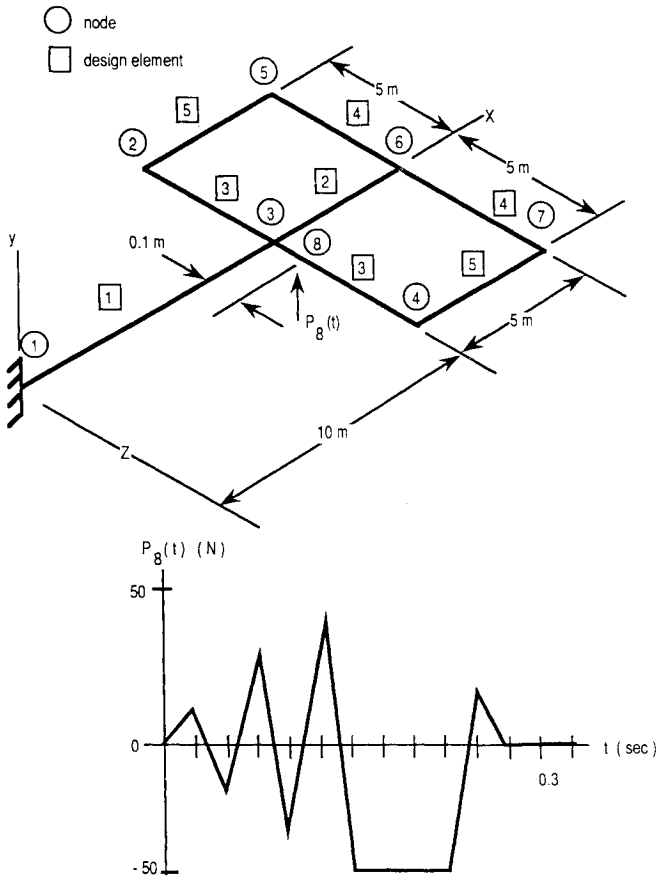

Fig. 4 Planar grillage example 21 degrees of freedom.

Planar Grillage Structure—Case 2

The minimum weight design of the planar grillage structure is sought where constraints are placed on the peak transient accelerations at nodes 2, 4, 5, 6, and 7, in addition to the constraints on peak transient displacements considered previously. Furthermore, spherical nonstructural mass design elements are used to represent the mass of sensor/actuator pairs plus any necessary vibration tuning mass. Each nonstructural mass design element has a density of $\rho = 2770$ kg/m^3, with the initial radius set equal to a lower bound value of 0.10 m (initial mass of 11.6 kg). The 11.6 kg (lower bound) mass is used to represent the fixed mass of the sensor/actuator pair and any additional mass represents vibration tuning mass found by the design procedure.

Optimum designs are sought for the uncontrolled structure, for the controlled structure using three type II sensor/actuator pairs at nodes 2, 4, and 6, and for the controlled structure using four type II sensor/actuator pairs located at nodes 2, 4, 5, and 7.

The optimum design for the uncontrolled transient displacement and transient acceleration constrained grillage structure is given in Table 3. The critical constraints at the optimum design are the peak dynamic displacement constraints at nodes 5 and 7 and the peak acceleration constraints at nodes 2, 4, and 6. This combination of critical constraints suggests that the structure acts predominantly like a cantilever beam without significant torsional effects.

Optimum designs for the type II controlled planar grillage structure can be found in Table 3. Three type II actuators lead to an optimum design with a total mass that is 31.1% lighter than the uncontrolled optimum design. Four type II actuators yield an optimum design with a total mass that is 30.7% lighter than the uncontrolled optimum design. For both of the type II controlled cases, the optimum design resembles a torsional mass damper and all of the actuator force levels fall between 8.27 and 6.95 N.

If the mass penalty assigned to each actuator were lower, then the mass saving achieved by introducing the fourth actuator could exceed the mass increase associated with adding it. Furthermore, if the loading function excited higher modes that had to be retained in the dynamic response calculations, it might be necessary to utilize additional actuators to control these extra modes.

This planar grillage structure example problem illustrates the beneficial effect that the addition of a control system can have on the resulting optimum design when forethought is given to the use and placement of the actuators. By judicious placement of the actuators, the primary modes participating in the response can be controlled with relatively low actuator output force levels, leading to lighter optimum designs in spite of the deliberately heavy weight penalty assigned to each sensor/actuator pair.

Planar Grillage Structure—Case 3

The third example problem is the minimum control effort design of the planar grillage shown in Fig. 4, subject to a mass cap of 400 kg. All other constraints and problem parameters are the same as the case 1 design problem. In addition, the same control law/actuator location combinations used in case 1 are used here.

Optimum designs for the type II controlled planar grillage are shown in Table 4. The initial design is highly infeasible (200%) with respect to the upper bound mass constraint, so the early iterations in the design process are concerned with finding a feasible design. Once a feasible design is found, the design either converges or decreases the effort and then converges to the optimum.

With a single actuator, bending effects are sufficiently controlled, resulting in torsional effects driving the final design. The addition of a second actuator allows both bending and torsional effects to be controlled, resulting in a 45% improvement in the effort objective function.

Table 3 Grillage structure optimal designs—case 2 (Type II actuators)

Design variables	Units	Uncontrolled (2A)	3 Type II actuators (2D)	4 Type II actuators (2E)
Beam 1 t	m	0.0046	0.0011	0.0012
Beam 2 t	m	0.0016	0.0011	0.0014
Beam 3 t	m	0.0020	0.0010	0.0011
Beam 4 t	m	0.0014	0.0011	0.0012
Beam 5 t	m	0.0018	0.0024	0.0016
Node 2 r	m	—	0.130	0.131
Node 4 r	m	—	0.129	0.124
Node 5 r	m	—	—	0.105
Node 6 r	m	—	0.107	—
Node 7 r	m	—	—	0.102
Node 2 ϵ	m/s	—	0.0034	0.0046
Node 2 $\bar{u}$	N	—	7.29	7.31
Node 4 ϵ	m/s	—	0.0042	0.0032
Node 4 $\bar{u}$	N	—	7.04	7.41
Node 5 ϵ	m/s	—	—	0.0024
Node 5 $\bar{u}$	N	—	—	7.28
Node 6 ϵ	m/s	—	0.0032	—
Node 6 $\bar{u}$	N	—	8.27	—
Node 7 ϵ	m/s	—	—	0.0023
Node 7 $\bar{u}$	N	—	—	6.95
Structural mass	kg	586	339	332
Total mass	kg	586	404	406
Iterations		16	16	14
Critical constraints		$X_{y5}, X_{y7}, \ddot{X}_{y2}$ $\ddot{X}_{y4}, \ddot{X}_{y6}$	t_3^-,[a] $X_{y7}, \ddot{X}_{y5}$	r_7^-,[b] $\ddot{X}_{y4}$

[a] $^-$:Design variable at lower bound. [b] Subscript on r indicates nodal locations.

Table 4 Planar grillage optimal designs—case 3 (Type II actuators)

Design variables	Units	1 Type II actuator (3C)	2 Type II actuators (3D)
Beam 1 t	m	0.0035	0.0031
Beam 2 t	m	0.0012	0.0010
Beam 3 t	m	0.0010	0.0013
Beam 4 t	m	0.0011	0.0012
Beam 5 t	m	0.0010	0.0012
Node 5 ϵ	m/s	—	0.0046
Node 5 $\bar{u}$	N	—	4.08
Node 6 ϵ	m/s	0.0051	—
Node 6 $\bar{u}$	N	8.20	—
Node 7 ϵ	m/s	—	0.0044
Node 7 $\bar{u}$	N	—	4.09
Control effort	$N^2 - s$	12.75	7.06
Iterations	—	18	20
Critical constraints	—	t_5^-,[a] W, X_{y6}, X_{y7}	$t_2^-, W, X_{y5}, X_{y6}, X_{y7}$

[a] $^-$:Design variable at lower bound.

In both of these cases, the resultant optimum designs have large primary load-carrying members (design element 1) and near-lower-bound remaining members. This material distribution suggests that a cantilever-type design is best for effort minimization when only displacement behavior constraints are present.

Planar Grillage Structure—Case 4

The final planar grillage design problem is a minimum control effort design with a 525 kg upper bound on the total system mass. The displacement and acceleration constraints imposed on the case 2 design problem are imposed here. All

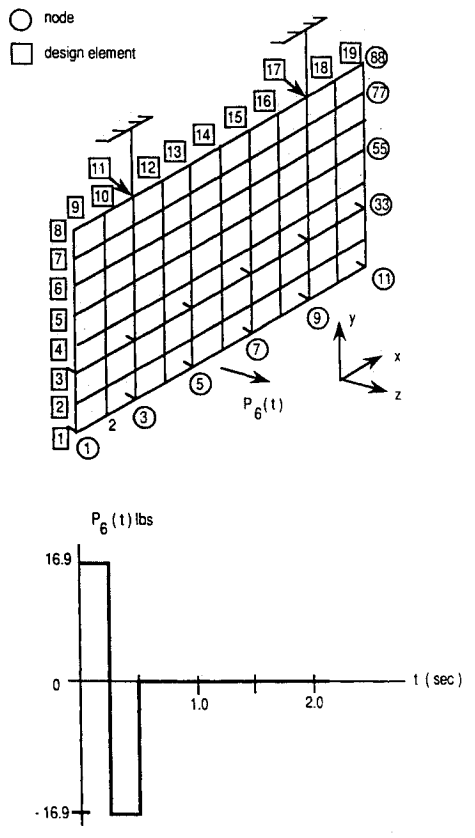

Fig. 5 Large grillage structure example.

other problem parameters and control configurations are the same as for the case 2 design problem.

Optimum designs for the type II controlled planar grillage design problem are given in Table 5. As was seen when only the displacement constraints were used in case 3, the early stages of the design procedure are spent trying to regain feasibility with respect to the upper bound mass constraint. Once the mass constraint is satisfied, the design procedure turns to reducing the effort objective function. From Table 5 it can be seen that the three type II controlled optimum design resemble a torsional vibration damper with the outboard members (design element 5) approximately the same size as the primary load-carrying members. On the other hand, the four type II controlled optimum design has the form of a cantilever tapering down from root to tip. These designs suggest that the structural design variables are tailored to satisfy acceleration constraints, whereas the control design variables are chosen to meet displacement constraints. In addition, adding a fourth actuator results in a 61% reduction in the minimum control effort objective function value achieved.

Table 5 Grillage structure optimal designs—case 4 (Type II actuators)

Design variables	Units	3 Type II actuators (4C)	4 Type II actuators (4D)
Beam 1 t	m	0.0024	0.0029
Beam 2 t	m	0.0014	0.0019
Beam 3 t	m	0.0020	0.0011
Beam 4 t	m	0.0016	0.0013
Beam 5 t	m	0.0021	0.0011
Node 2 r	m	0.106	0.133
Node 4 r	m	0.104	0.126
Node 5 r	m	—	0.100
Node 6 r	m	0.103	—
Node 7 r	m	—	0.100
Node 2 ϵ	m/s	0.0046	0.0050
Node 2 $\bar{u}$	N	5.72	3.70
Node 4 ϵ	m/s	0.0045	0.0041
Node 5 $\bar{u}$	N	6.28	3.41
Node 5 ϵ	m/s	—	0.0064
Node 5 $\bar{u}$	N	—	5.14
Node 6 ϵ	m/s	0.0032	—
Node 6 $\bar{u}$	N	7.03	—
Node 7 ϵ	m/s	—	0.0072
Node 7 $\bar{u}$	N	—	4.81
Control effort	N^2-s	17.15	6.50
Iterations		16	17
Critical constraints		r_6^-,[a,b] W	r_5^-, r_7^-, W

[a] $^-$:Design variable at lower bound. [b]Subscript on r indicate nodal locations.

Table 6 Grillage structure input data

Material properties:	$E=10.5\times10^6$ psi $\rho=0.1$ lb/in.^{3} $\nu=0.3$
Dynamic loading:	(See Fig. 5)
Dynamic constraints:	$\lvert X_{z1}\rvert \le 2.5$ in. $\lvert X_{z11}\rvert \le 2.5$ in. $\lvert X_{z78}\rvert \le 2.5$ in. $\lvert X_{z88}\rvert \le 2.5$ in.
Control constraints:	$E \le 10.0$ lb$^2-$s
CSD variable linking:	$B=2t_3=$ fixed, $H=2t_2$ $\epsilon=30.0$ in./s fixed (Type I only)

Side constraints

Variable	Units	Lower bound	Initial design	Upper bound
B	in.	1.00	2.00	3.00
H	in.	0.10	0.25	0.50
t_2	in.	0.05	0.125	0.25
t_3	in.	0.50	1.00	1.50
δ	in.	0.01	3.00	10.00
ϵ	in./s	1.00	40.00	90.00
$\bar{u}$	lb	0.01	0.80	10.0

Large Grillage Structure

The final optimum design problem presented here is the minimum weight design of the 264-degree-of-freedom grillage structure shown in Fig. 5. The grillage is cantilevered from two fixed supports and is made up of 19 aluminum beams with 2.0 in. widths and initial heights of 0.25 in. The external load time history, meant to represent the loads placed on the grillage during a spacecraft slew maneuver,[2] is applied at node 6. An upper bound of 2.5 in. is imposed on the peak dynamic displacements at the four corners of the grillage structure. Dynamic response calculations were done using 20 retained modes (frequency content up to 100 Hz), a final integration time of 1.0 s, a time step size of 0.0005 s, and 2% modal damping (i.e., $\zeta=0.02$). All pertinent information for this problem is given in Table 6.

Three minimum weight design subcases are documented here: 1) the uncontrolled grillage; 2) the 12 actuator type I controlled grillage; and 3) the 12 actuator type II controlled grillage. For all controlled subcases, the sensor/actuator pairs are uniformly distributed along design elements 1 and 3 (see Fig. 5) and have a fixed nonstructural weight of 0.5 lb.

The optimum design for the uncontrolled grillage structure is shown in Table 7. The minimum weight attained is 57.96 lb, with the height of all members approaching their lower bounds except for the primary load-carrying members (design elements 8, 11, and 17), which have grown from their initial values (0.25 in.).

Table 7 Grillage structure optimal designs Structural variables

Design variables	Units	Uncontrolled (5A)	12 Type II actuators (5B)	12 Type II actuators (5C)
Beam 1 H	in.	0.100	0.100	0.100
Beam 2 H	in.	0.100	0.100	0.100
Beam 3 H	in.	0.100	0.100	0.100
Beam 4 H	in.	0.100	0.100	0.100
Beam 5 H	in.	0.100	0.100	0.100
Beam 6 H	in.	0.100	0.100	0.100
Beam 7 H	in.	0.125	0.127	0.100
Beam 8 H	in.	0.311	0.218	0.100
Beam 9 H	in.	0.100	0.118	0.100
Beam 10 H	in.	0.100	0.116	0.100
Beam 11 H	in.	0.398	0.370	0.286
Beam 12 H	in.	0.131	0.144	0.100
Beam 13 H	in.	0.100	0.100	0.100
Beam 14 H	in.	0.100	0.100	0.100
Beam 15 H	in.	0.100	0.100	0.100
Beam 16 H	in.	0.100	0.109	0.100
Beam 17 H	in.	0.417	0.345	0.282
Beam 18 H	in.	0.124	0.129	0.100
Beam 19 H	in.	0.100	0.111	0.100
Structural weight	lb	57.96	54.83	46.15
Total weight	lb	57.96	60.83	52.15
Iterations		14	12	12
Critical constraints		H_1^-,[a]H_2^-,H_3^- H_4^-,H_5^-,H_6^- H_9^-,H_{10}^-,H_{13}^- H_{14}^-,H_{15}^-,H_{16}^- H_{19}^-,X_{z1},X_{z11}	H_1^-,H_2^-,H_3^- H_4^-,H_5^-,H_6^- H_{13}^-,H_{14}^-,H_{15}^- X_{z1},X_{z11}	H_1^-,H_2^-,H_3^- H_4^-,H_5^-,H_6^- H_7^-,H_8^-,H_9^- H_{10}^-,H_{12}^-,H_{13}^- H_{14}^-,H_{15}^-,H_{16}^- H_{18}^-,H_{19}^-,E^- X_{z1},X_{z11}

[a] $^-$:Design variable at lower bound.

Table 8 Grillage structure optimal designs Control variable

Design variables	Units	Uncontrolled (5A)	12 Type I actuators (5B)	12 Type II actuators (5D)
Node 1 ϵ	in.*	—	1.071	15.64
Node 1 $\bar{u}$	lb	—	1.549	1.439
Node 3 ϵ	in.*	—	0.958	8.07
Node 3 $\bar{u}$	lb	—	1.068	1.565
Node 5 ϵ	in.*	—	0.937	10.36
Node 5 $\bar{u}$	lb	—	1.048	1.437
Node 7 ϵ	in.*	—	0.930	10.31
Node 7 $\bar{u}$	lb	—	1.033	1.436
Node 9 ϵ	in.*	—	0.917	8.07
Node 9 $\bar{u}$	lb	—	1.037	1.565
Node 11 ϵ	in.*	—	1.040	14.60
Node 11 $\bar{u}$	lb	—	1.431	1.450
Node 23 ϵ	in.*	—	0.784	35.00
Node 23 $\bar{u}$	lb	—	1.242	0.444
Node 25 ϵ	in.*	—	2.151	35.00
Node 25 $\bar{u}$	lb	—	0.782	0.565
Node 27 ϵ	in.*	—	2.434	35.00
Node 27 $\bar{u}$	lb	—	0.766	0.431
Node 29 ϵ	in.*	—	2.433	35.00
Node 29 $\bar{u}$	lb	—	0.766	0.430
Node 31 ϵ	in.*	—	2.148	35.00
Node 31 $\bar{u}$	lb	—	0.782	0.505
Node 33 ϵ	in.*	—	0.778	35.00
Node 33 $\bar{u}$	lb	—	1.148	0.464

[a] in.* = δ and in. for Type I, ϵ and in./s for Type II.

The addition of type I actuators to the large grillage structure results in a 5.4% structural weight savings when compared with the uncontrolled optimum design (see Tables 7 and 8), but a 4.9% total weight penalty. The higher total weight for the type I controlled grillage is a result of the type I controllers inability to pay for themselves (in terms of assigned weight) in this design problem.

On the other hand, the use of type II controllers on the large grillage structure results in both a structural weight savings (20.4%) and a total weight savings (10.0%) when compared with the uncontrolled optimum design. At the optimum design for case 5C, the dynamic displacement constraints at nodes 1 and 11 and the control effort upper bound drive the design. As a result of the effort upper bound becoming critical, the design procedure attempts to find the most efficient actuator locations for controlling dynamic response while satisfying the upper bound effort constraint. For the grillage structure shown in Fig. 5, this was accomplished by completely turning off the inside row of actuators along design element 3 (i.e., raising their velocity threshold high enough so that they never get turned on) and allowing the actuators located at nodes 3 and 9 (where the primary load-carrying members are) to expend the most effort.

Concluding Remarks

The control augmented structural sythesis approach has been successfully extended to systems involving general transient response and nonlinear on/off controllers. An important feature of this work is that limitations on dynamic response and actuator force levels are met by treating them as direct behavior constraints, rather than by incorporating them into a system performance index. Herein the integrated structures/control system design problem was first formulated as a nonlinear mathematical programming problem involving time parametric constraints. Solutions were then obtained by solving a sequence of explicit approximate NLP problems. These approximate problems were constructed by first replacing the time parametric constraints with a finite number of regular constraints corresponding to response peaks, and then using hybrid approximations to generate explicit representations of these constraints in terms of the independent design variables. The efficiency of the dynamic response sensitivity analysis was improved significantly by applying the Wilkie-Perkins essential parameter method. The optimization procedure also incorporates design variable linking and constraint deletion features. Numerical results for example problems that exhibit characteristics representative of more complex systems indicate that substantial improvement can be achieved through integrated design optimization of structures and controls. Furthermore, the integrated structures/controls design optimization procedure presented here can identify the most efficient locations for control actuators by deactivating those actuators that are poorly located for controlling dynamic response.

Acknowledgments

This research was supported by NASA Research Grant NSG-1490.

References

[1]Horner, G. C., "Optimum Actuator Placement, Gain, and Number for a Two-Dimensional Grillage," *Proceedings of the 24th AIAA/ASME/ASCE/AHS Structures, Structural Dynamics, and Materials Conf.*, AIAA, New York, May 1983, pp. 179–184.

[2]Horner, G. C., and Walz, J. E., "A Design Technique for Determining Actuator Gains in Spacecraft Vibration Control," *Proceedings of the 26th AIAA/ASME/ASCE/AHS Structures, Structural Dynamics, and Materials Conf.*, AIAA, New York, April 1985, pp. 143–151.

[3]Oz, H., and Meirovitch, L., "Optimal Modal Space Control of Flexible Gyroscopic Systems," *Journal of Guidance, Control, and Dynamics*, Vol. 3, May–June 1980, pp. 218–226.

[4]Haftka, R. T., Martinovic, Z. N., and Hallauer, W. L., "Enhanced Vibration Controllability by Minor Structural Modifica-

tions," *Proceedings of the 25th AIAA/ASME/ASCE/AHS Structures, Structural Dynamics, and Materials Conf.*, AIAA, New York, May 1984, pp. 401-410.

[5]Venkayya, V. B., and Tischler, V. A., "Frequency Control and the Effect on the Dynamic Response of Flexible Structures," *Proceedings of the 25th AIAA/ASME/ASCE/AHS Structures, Structural Dynamics, and Materials Conf.*, AIAA, New York, May 1984, pp. 431-441.

[6]Khot, N. S., Eastep, F. E., and Venkayya, V. B., "Optimal Simultaneous Structural and Control Design of Maneuvering Flexible Spacecraft," *Journal of Guidance, Control, and Dynamics,* Vol. 8, No. 1, Jan.-Feb. 1985, pp. 86-93.

[7]Messac, A., and Turner, J., "Dual Structural-Control Optimization of Large Space Structures," NASA-CP 2327 (Part 2), April 1984, pp. 775-802.

[8]Junkins, J. L., Bodden, D. S., and Turner, J. D., "A Unified Approach to Structure and Control System Design Iterations," Fourth International Conf., on Applied Numerical Modeling, Tainan, Taiwan, Dec. 1984.

[9]Bodden, D. S., and Junkins, J. L., "Eigenvalue Optimization Algorithms for Structure/Controller Design Iterations," *Journal of Guidance, Control, and Dynamics,* Vol. 8, No. 6, Nov.-Dec. 1985, pp. 697-706.

[10]Khot, N. S., Oz, H., Grandhi, R. V., Eastep, F. E., and Venkayya, V. B., "Optimal Structural Design with Control Gain Norm Constraint," *AIAA Journal,* Vol. 26, May 1988, pp. 604-611.

[11]Belvin, W. K., and Park, K. C., "Structural Tailoring and Feedback Control Synthesis: An Interdisciplinary Approach," *Proceedings of the 29th AIAA/ASME/ASCE/AHS Structures, Structural Dynamics, and Materials Conf.*, AIAA, Washington, DC, April 1988, pp. 1-8.

[12]Rao, S. S., Venkayya, V. B., and Khot, N. S., "Game Theory Approach for the Integrated Design of Structures and Control," *AIAA Journal,* Vol. 26, April 1988, pp. 463-469.

[13]Lust, R. V., and Schmit, L. A., "Control Augmented Structural Synthesis," *AIAA Journal,* Vol. 26, Jan. 1988, pp. 463-469.

[14]Lust, R. V., and Schmit, L. A., "Alternative Approximation Concepts for Space Frame Synthesis," NASA-CR 172526, March 1985.

[15]Starnes, J. H., Jr., and Haftka, R. T., "Preliminary Design of Composite Wings for Buckling, Stress, and Displacement Constraints," *Journal of Aircraft,* Vol. 16, Aug. 1979, pp. 564-570.

[16]Vanderplaats, G. N., "CONMIN—A Fortran Program for Constrained Function Minimization," NASA-TM X-62, 282, Aug. 1973.

[17]Meirovitch, L., *Analytical Methods in Vibrations,* MacMillan, New York, 1967.

[18]Bathe, K., and Wilson, E. L., *Numerical Methods in Finite Element Analysis,* Prentice Hall, Englewood Cliffs, NJ, 1976.

[19]Wilkie, D. F., and Perkins, W. R., "Essential Parameters in Sensitivity Analysis," *Automatica,* Vol. 5, 1969, pp. 191-197.

[20]Manning, R. A., Lust, R. V., and Schmit, L. A., "Behavior Sensitivities for Control Augmented Structures," NASA-CP 2457, 1987, pp. 33-57.

[21]Manning, R. A., "Control Augmented Structural Synthesis with Transient Response Constraints," Ph.D. Dissertation, Univ. of California, Los Angeles, CA, 1987.